Wright, and R. C. Keezer, Solid State Commun. 5, 113 (1967).

[22]I. Chen and R. Zallen, Phys. Rev. 173, 833 (1968).

PHYSICAL REVIEW B VOLUME 5, NUMBER 2 15 JANUARY 1972

# A Consistency Test for X-Ray Form Factors

A. Marcus Gray
*Watervliet Arsenal, Watervliet, New York* 12180
(Received 11 June 1971)

The validity of electronic band-structure results may be tested by comparing the Fourier transforms of the electronic charge distribution with x-ray structure factors. Measurement of the latter is difficult and liable to relatively large errors. If more than one published set exists it is sometimes difficult to decide which is the most reliable. A simple model for the electronic charge distribution in cubic crystals is proposed, and hence a parametrized expression for x-ray form factors is derived. This is fitted to the available sets of measured form factors by a least-squares technique, giving an indication of the consistency of each set and thus its reliability. Experimental data for Al, diamond, and Si are examined by this method. Electron distributions are drawn in {100} and {110} planes.

## I. INTRODUCTION

A possible method of checking the validity of theoretical band-structure calculations is by comparing the Fourier transforms of the calculated electronic charge distribution with measured x-ray structure factors. However, the derivation of structure factors by experiment is subject to many corrections and the best precision that can presently be obtained is of the order of 1%.[1] Different sets of measurements may show considerable disagreement among each other and it is sometimes difficult to decide which set to use for the comparison with band-structure results.

A simple parametrized theoretical model for the electronic charge distribution in cubic solids is proposed here, and hence a theoretical form-factor expression is derived. The consistency of several sets of measurements is then tested by means of a least-squares fitting procedure.

The approach differs from the conventional use of x-ray diffraction measurements in that the symmetry of the crystal is assumed to be known at the outset.

## II. MODEL CHARGE DISTIRBUTION AND FORM FACTORS

The electron distribution in the crystal $\rho_c(\vec{r})$ can be expressed as

$$\rho_c(\vec{r}) = \sum_{\vec{K}} \hat{\rho}_c(\vec{K})\, e^{-i\vec{K}\cdot\vec{r}} \ , \tag{1}$$

where

$$\hat{\rho}_c(\vec{K}) = \frac{1}{\Omega}\int \rho_c(\vec{r})\, e^{i\vec{K}\cdot\vec{r}}\, d\tau \tag{2}$$

and integration is over the volume of the primitive cell $\Omega$. $\vec{K}$ are reciprocal-lattice vectors. $\rho_c(\vec{r})$ can also be expressed as a superposition of localized charge distributions:

$$\rho_c(\vec{r}) = \sum_{i,j} \rho_s^j(\vec{r} - \vec{\tau}_j - \vec{R}_i), \tag{3}$$

where $\vec{\tau}_j$ fixes the position in the primitive cell, $\vec{R}_i$ is the cell, and where the $\rho_s^j$ are designated as "site distributions." The superscript $j$ distinguishes the different site distributions associated with a primitive cell containing a basis.

Substituting Eq. (3) into Eq. (2) and making the substitutions $\vec{r} - \vec{\tau}_j - \vec{R}_i = \vec{r}'$ results in

$$\hat{\rho}_c(\vec{K}) = \frac{1}{\Omega}\sum_j e^{i\vec{K}\cdot\vec{\tau}_j} \int \rho_s^j(\vec{r}')\, e^{i\vec{K}\cdot\vec{r}'}\, d\tau', \tag{4}$$

where now integration ranges over the extent of the site distribution which may extend beyond the cell boundary. The integral is equivalent to the x-ray form factor[2] $f_j(\vec{K})$ for a charge distirbution $\rho_s^j(\vec{r})$: We have

$$f_j(\vec{K}) = \int \rho_s^j(\vec{r})\, e^{i\vec{K}\cdot\vec{r}}\, d\tau \ , \tag{5}$$

so that

$$\hat{\rho}_c(\vec{K}) = \frac{1}{\Omega}\sum_j e^{i\vec{K}\cdot\vec{\tau}_j} f_j(\vec{K}) \equiv \frac{1}{\Omega}\, F(\vec{K}), \tag{6}$$

where $F(\vec{K})$ is the x-ray structure factor. Equation (6) demonstrates the relation between the Fourier transforms of the crystal charge density and the x-ray structure factors.

It should be noted that x-ray form factors are completely determined from the electron charge distribution and do not depend on the detailed wave-function behavior.

According to Eq. (5), the site charge distribution is the inverse Fourier transform of the form factor.

Since the form factors are only defined at reciprocal-lattice vectors in reciprocal space, the site distributions are not uniquely defined.[3]

Form factors derived from x-ray measurements in solids differ only slightly from atomic measurements calculated theoretically from wave functions. The difference is due to a redistribution of valence electrons.[4,5] In accordance with this idea, a site distribution is set up in which the valence electron distribution is parametrized, both radial and angular variation being possible. Since the crystal charge density has the symmetry of the crystal space group there are symmetry restrictions on the site distributions.[6] In the case of a symmorphic group, the site distribution has the symmetry of the point group. A radial cutoff parameter $D$ is introduced for $\rho_s^j(\vec{r})$ in order to avoid spurious fits. $D$ must be sufficiently large to allow a certain amount of overlap of the site distributions. In most cases, it was chosen to correspond to the radius to which atomic wave functions under consideration are tabulated. In every case the core distribution was assumed to be unchanged from the atom. The site distribution for the valence electrons has the following form:

$$\rho_s^j(\vec{r}) = \rho(r)\,(a_0 + a_1 r + a_2 r^2)\,\gamma_j(r,\theta,\phi) \quad \text{for } r < D, \tag{7}$$

$$\rho_s^j(\vec{r}) = 0 \quad \text{for } r \geq D,$$

$$\gamma_j(r,\theta,\phi) \equiv 1 + r\left(b_1 \frac{x^4+y^4+z^4}{r^4} + b_2 \frac{x^2y^2z^2}{r^6} \pm b_3 \frac{xyz}{r^3}\right). \tag{8}$$

Here $\rho(r)$ is the spherically symmetric atomic electron distribution calculated from tabulated wave functions. The quadratic term allows for radial variation, forming an envelope function for $\rho(r)$ forcing $\rho_s^j(\vec{r})$ to zero at $r = D$. The $r$ dependence in the angular term is introduced in order to allow for spherical symmetry in the vicinity of the nucleus. $b_3$ is nonzero only for the diamond structure; the plus sign applies for the site distribution at $\vec{r} = 0$, the minus for that at $\vec{r} = \frac{1}{4}a(111)$ in the primitive cell.

$a_0$, $b_1$, $b_2$, and $b_3$ are adjustable parameters. $a_1$ and $a_2$ are related to them by the cutoff value $D$ and the fact that the site distribution contains the same number of electrons as the atom:

$$a_1 = \frac{1 - a_0\{C_0 + (\frac{3}{5}b_1 + \frac{1}{105}b_2)\,C_1 - (1/D^2)\,[C_2 + (\frac{3}{5}b_1 + \frac{1}{105}b_2)\,C_3]\}}{C_1 + (\frac{3}{5}b_1 + \frac{1}{105}b_2)\,C_2 - (1/D)\,[C_2 + (\frac{3}{5}b_1 + \frac{1}{105}b_2)\,C_3]}. \tag{9}$$

where

$$C_n = \int_0^D r^n \rho\, d\tau \Big/ \int_0^\infty \rho\, d\tau, \tag{10}$$

$$a_2 = -(a_0 + a_1 D)/D^2. \tag{11}$$

An expression for the form factors $f_j(\vec{K})$ of $\rho_s^j$ is then derived. Depending on the symmetry of the site distribution it may be complex: We have

$$f_j(\vec{K}) \equiv \mathrm{Re} f_j(\vec{K}) + i\,\mathrm{Im} f_j(\vec{K}). \tag{12}$$

Only the tetrahedral term of Eq. (8) can give rise to an imaginary term. We have

$$\begin{aligned}\mathrm{Re} f_j(\vec{K}) = a_0[&\langle j\rangle_0 + b_1(\langle jr\rangle_4\,\chi_1 + \tfrac{3}{5}\langle jr\rangle_0) \\ &+ b_2(\langle jr\rangle_6\,\chi_2 - \tfrac{1}{22}\langle jr\rangle_4\,\chi_1 + \tfrac{1}{105}\langle jr\rangle_0)] \\ &+ a_1[\langle jr\rangle_0 + b_1(\langle jr^2\rangle_4\,\chi_1 + \tfrac{3}{5}\langle jr^2\rangle_0) \\ &+ b_2(\langle jr^2\rangle_6\,\chi_2 - \tfrac{1}{22}\langle jr^2\rangle_4\,\chi_1 + \tfrac{1}{105}\langle jr^2\rangle_0)] \\ &+ a_2[\langle jr^2\rangle_0 + b_1(\langle jr^3\rangle_4\,\chi_1 + \tfrac{3}{5}\langle jr^3\rangle_0) \\ &+ b_2(\langle jr^3\rangle_6\,\chi_2 - \tfrac{1}{22}\langle jr^3\rangle_4\,\chi_1 + \tfrac{1}{105}\langle jr^3\rangle_0)]\end{aligned} \tag{13}$$

and

$$\mathrm{Im} f_j(\vec{K}) = \mp b_3(a_0\langle jr\rangle_3 + a_1\langle jr^2\rangle_3 + a_2\langle jr^3\rangle_3)\,\chi_3, \tag{14}$$

where now the negative sign applies to the site distribution at $\vec{r} = 0$ and the positive sign applies to that at $\vec{r} = \frac{1}{4}a(111)$, and we obtain

$$\langle jr^n\rangle_l \equiv \int_0^D j_l(Kr)\,P^2 r^n\, dr, \tag{15}$$

where $j_l(Kr)$ is the spherical Bessel function of order $l$ and

$$P^2 = 4\pi r^2 a_B^3 \rho \tag{16}$$

with $a_B$ as the Bohr radius. We have

$$\chi_1 = (K_x^4 + K_y^4 + K_z^4)/K^4 - \tfrac{3}{5}, \tag{17}$$

$$\chi_2 = -K_x^2K_y^2K_z^2/K^6 - (K_x^4 + K_y^4 + K_z^4)/22K^4 + 17/462, \tag{18}$$

$$\chi_3 = K_xK_yK_z/K^3. \tag{19}$$

When fitting these expressions to experimental data it is best to restrict oneself to as few parameters as possible. Although the computer program was set up to allow variation of four independent parameters ($a_0$, $b_1$, $b_2$, and $b_3$) it was found, in practice, that the fitting was independent of the parameter $b_2$.

## III. MODIFICATIONS FOR COMPARISON OF MODEL FORM FACTORS WITH EXPERIMENTAL RESULTS

Experimental results for Al, diamond, and Si, tabulated in the form of form factors, are considered. Room-temperature results are reduced to $T = 0\,^{\circ}\mathrm{K}$ by means of the Debye-Waller formula

$$f_T(\vec{K}) = f_0(\vec{K})\, e^{-BK^2}, \tag{20}$$

where $f_T(\vec{K})$ and $f_0(\vec{K})$ are the room-temperature and $T = 0\,^{\circ}\mathrm{K}$ are form factors, respectively. The assumption is made that at relatively large $\vec{K}$, $f_0(\vec{K}) = \langle j\rangle_0$. $B$ is then found by a least-squares fitting to

$$\ln(\langle j\rangle_0 / f_T) = BK^2 \tag{21}$$

and substituted into the transposed Eq. (20) to obtain $f_0(\vec{K})$.

The fcc lattice contains one atom per primitive cell and thus we have

$$F(\vec{K}) = f(\vec{K}), \tag{22}$$

where the subscript $j$ of the model form factor can now be omitted. The expression for the model form factors $f(\vec{K})$ is fitted to the experimental values $f_0(\vec{K})$.

In case of crystals of the diamond structure, the tabulated quantities $f_0(\vec{K})$ are not true form factors. They are defined by

$$\left|F(\vec{K})\right| = 2 f_0(\vec{K}) \left|\cos \tfrac{1}{2}\vec{K}\cdot\vec{\tau}\right| . \tag{23}$$

The absolute structure factor expressed in terms of the complex form factor is

$$\left|F(\vec{K})\right| = 2\left|\,\mathrm{Re} f(\vec{K}) \cos \tfrac{1}{2}\vec{K}\cdot\vec{\tau} + \mathrm{Im} f(\vec{K})\, \sin \tfrac{1}{2}\vec{K}\cdot\vec{\tau}\right| , \tag{24}$$

where $f(\vec{K})$ is the true form factor for the site distribution at $\vec{r} = 0$, the other site being at $\vec{r} = \frac{1}{4}a(111)$.

Equating Eqs. (23) and (24) one finds

$$f_0(\vec{K}) = \left|\,\mathrm{Re}\, f(\vec{K}) + \tan \tfrac{1}{2}\vec{K}\cdot\vec{\tau}\, \mathrm{Im}\, f(\vec{K})\right| . \tag{25}$$

In the case of the proposed model, $\mathrm{Re} f(\vec{K})$ and $\mathrm{Im} f(\vec{K})$ are given by Eqs. (13) and (14), respectively. This expression for $f_0(\vec{K})$ is then fitted to the experimental values by means of a least-squares procedure. Since products of parameters occur, a nonlinear procedure is called for; this results in several solutions with almost equal standard deviations.

In the case of forbidden reflections $\frac{1}{2}\vec{K}\cdot\vec{\tau}$ is an odd multiple of $\frac{1}{2}\pi$ and

$$\left|F(\vec{K})\right| = 2\left|\mathrm{Im} f(\vec{K}) \sin \tfrac{1}{2}\vec{K}\cdot\vec{\tau}\right| . \tag{26}$$

According to the proposed model, $\mathrm{Im} f(\vec{K})$ depends on $b_3$. Since forbidden reflections have been detected for Si and diamond, the term in $b_3$ cannot be omitted when fitting to form factors of allowed reflection for those crystals.

## IV. EMPIRICAL ERROR BOUNDS

The parameters of Eqs. (13) and (14) giving the best least-squares fit to experimental form factors are found. The corresponding model form factors and their standard deviation from the experimental set $\sigma$ are then evaluated. $\sigma$ serves as the criterion of the consistency of the measured set.

It seems desirable to estimate how the uncertainty in the experimental results as well as the choice of model affect the precision of the calculated parameters, thus giving a measure of their significance. To this end the model form factors are randomly perturbed using a Gaussian distribution with a standard deviation equal to $\sigma$ calculated above. A new fit is then obtained to these perturbed model form factors producing a new set of parameters and model form factors. This perturbation procedure is applied 30 times in the case of Al and 10 times in case of diamond and Si. Standard deviations for each parameter, each form factor, and the forbidden reflections are then calculated; these are the quantities in parentheses in Tables I–III. To run the entire procedure for Al, fitting to 9 form factors, takes about 10 min of computer time.[7] Diamond fitting to 23 form factors takes about 14 min.

## V. CRYSTAL CHARGE DISTRIBUTION

Once the parameters have been determined it is a simple matter to form the crystal charge distribution by superposition of the site distributions.

TABLE I. Consistency of two sets of experimental x-ray form factors for Al. All data are for $T = 0\,^{\circ}\mathrm{K}$. The effect of different models is examined by choosing two different cutoff values $D$. No adjustable parameters are used.

| | Form factors | | | | |
|---|---|---|---|---|---|
| | Atom[a] | | Model | Model | |
| $hkl$ | HF | Expt.[b] | $D = 5.26a_B$ | $D = 26.95a_B$ | Expt.[a] |
| 111 | 9.03 | 8.80±0.06 | 8.85 | 8.79 | 8.70 |
| 200 | 8.60 | 8.38±0.06 | 8.39 | 8.42 | 8.31 |
| 220 | 7.37 | 7.27±0.06 | 7.28 | 7.33 | 7.17 |
| 311 | 6.69 | 6.66±0.06 | 6.63 | 6.66 | 6.59 |
| 222 | 6.60 | 6.48±0.06 | 6.45 | 6.46 | 6.52 |
| 400 | 5.70 | 5.78±0.06 | 5.75 | 5.74 | 5.77 |
| 331 | 5.29 | 5.33±0.06 | 5.28 | 5.28 | 5.34 |
| 420 | 5.10 | 5.20±0.05 | 5.14 | 5.14 | 5.20 |
| 422 | 4.60 | 4.66±0.05 | 4.65 | 4.63 | 4.71 |
| Standard deviation | | 0.03, 0.04 | | | 0.11, 0.11 |
| $a_0$ | | | 0 | 0 | |
| $a_1(a_0, D)a_B^{-1}$ | | | 0.9398 | 0.3978 | |
| $a_2(a_0, D)a_B^{-2}$ | | | −0.1785 | −0.01476 | |

[a]Reference 4. [b]Reference 10.

TABLE II. Consistency of two sets of experimental x-ray form factors for diamond. Empirical confidence bounds on fitted values are shown in parentheses. All data are for $T = 0$ °K. Three adjustable parameters were used; the fit was made to 23 values in each case; however, only the first 9 are shown here. $D = 12.4a_B$ for the model charge density cutoff value. $F(hkl)$ is the structure factor per primitive cell for a forbidden reflection. Comparison with band-structure results is made.

| | | | Form factors | | | |
|---|---|---|---|---|---|---|
| $hkl$ | Atom RHF[a] | Band-structure[a] | Expt.[b] | Fit | Expt.[c] | Fit |
| 111 | 3.03 | 3.30 | 3.321±0.007 | 3.32(0.02) | 3.341 | 3.34(0.07) |
| 220 | 1.96 | 1.95 | 1.972±0.009 | 1.97(0.01) | 1.865 | 1.86(0.03) |
| 311 | 1.76 | 1.66 | 1.662±0.007 | 1.67(0.01) | 1.567 | 1.56(0.02) |
| 400 | 1.59 | 1.53 | 1.479±0.009 | 1.50(0.02) | 1.474 | 1.45(0.06) |
| 331 | 1.52 | 1.53 | 1.579±0.005 | 1.57(0.01) | 1.486 | 1.55(0.02) |
| 422 | 1.44 | 1.41 | 1.443±0.002 | 1.44(0.00) | 1.286 | 1.43(0.01) |
| 511 | 1.40 | 1.37 | 1.418±0.005 | 1.37(0.01) | 1.342 | 1.36(0.02) |
| 333 | 1.40 | 1.34 | 1.418±0.005 | 1.39(0.01) | 1.319 | 1.37(0.02) |
| 440 | 1.33 | 1.31 | 1.287±0.009 | 1.33(0.00) | 1.276 | 1.32(0.01) |
| Standard deviation | | | | 0.02 | | 0.05 |
| $\lvert F(222)\rvert$ | | 0.24 | 0.30[d] | 0.19(0.04) | | 0.3(0.1) |
| $\lvert F(622)\rvert$ | | | 0.00[d] | 0.006(0.001) | | 0.005(0.003) |
| $a_0$ | | | | 0.37(0.04) | | −0.1(0.1) |
| $a_1(a_0,\ b_1,\ b_3)\ a_B^{-1}$ | | | | 0.91(0.09) | | 1.4(0.3) |
| $a_2(a_0,\ b_1,\ b_3)\ a_B^{-2}$ | | | | −0.076(0.007) | | −0.11(0.03) |
| $b_1$ $a_B^{-1}$ | | | | −0.32(0.03) | | −0.3(0.1) |
| $b_3$ $a_B^{-1}$ | | | | 0.7(0.2) | | 1.1(0.8) |

[a]Reference 1. [b]Reference 13. [c]Reference 14. [d]Reference 15.

Conventional methods for evaluating the crystal charge distribution from x-ray measurements[3,8,9] are (i) straightforward evaluation of three-dimensional Fourier series, representing higher-order terms by theoretical atomic form factors, and (ii) the method of convolution. The present method is an extension of (ii). In the original application[3] a smooth curve is drawn through the $f_0(\vec{K})$-vs-$|\vec{K}|$ plot. This curve is then fitted by a sum of Gaussians making it convenient to calculate the corresponding portion of the site distribution by means of a Fourier transformation. A correction is then added in the form of a Fourier series having as coefficients the deviation of the measured points from the smooth curve. Points will lie off the smooth curve whenever the site distribution is nonspherical. In the present treatment, the fit is made directly to the points $f_0(\vec{K})$, thus making allowance for nonspherical site distributions and eliminating the necessity of adding a Fourier series. The charge distribution in the core region is fixed in a more satisfactory way than with former methods. To estimate the effect of an inaccurate representation in the core region on the calculated charge distribution in the remainder of the crystal would involve a considerable amount of computation and was not investigated at this time.

Computer time for generating the crystal charge distribution from site distributions is very dependent on the choice of $D$. A decrease in $D$ substantially decreases the computer time, e.g., the case of Al generating $16\times 8$ points in the $\{110\}$ planes with $D = 5.26a_B$ takes 1 min, while with $D = 26.95a_B$ this takes 9 min. It is valid to vary $D$ because, as indicated above, the choice of site distribution is not unique.

## VI. RESULTS

The proposed model was fitted to experimental form factors for Al, diamond, and Si. Results are given in Tables I–III.

Some of the very recent experiments[1,10] appear to be considerably more accurate than previous data. These results make it possible to determine the parameters that should be retained in the model. In the case of Al, the model expression (13) was fitted for two different cutoff values: $D = 5.26a_B$, the smallest radius that still produces reasonable overlap of site distributions, and $D = 26.95a_B$, the radius to which the atomic wave functions are tabulated. In both cases the model was found to be independent of the parameters $a_0$, $b_1$, $b_2$, and $b_3$. Setting these parameters equal to zero results in a good fit of the model to the experimental form factor of Raccah and Henrich[10] for either value of $D$. Eight of the nine model form factors lie within their listed experimental error; $f(420)$ falls outside by 0.01. For both values of $D$ the model indicates a slight outward radial displacement of the valence charge in going from the atomic to the metallic

TABLE III. Consistency of two sets of experimental x-ray form factors for Si. Empirical condidence bounds on fitted values are shown in parentheses. All data are for $T=0$ °K. Three adjustable parameters were used; the fit was made to 10 form factors of Ref. a and to 22 form factors of Ref. b. $D=26.3a_B$ for the model charge density cutoff value. $F(hkl)$ is the structure factor per primitive cell for a forbidden reflection. Comparison with band-structure results is made.

| | | Form factors | | | | |
|---|---|---|---|---|---|---|
| *hkl* | Atom RHF[a] | Band-structure[a] | Expt.[a] | Fit | Expt.[b] | Fit |
| 111 | 10.53 | 10.88 | 11.12±0.04 | 11.12(0.02) | 10.89 | 10.98(0.12) |
| 220 | 8.71 | 8.76 | 8.78±0.09 | 8.78(0.02) | 8.77 | 8.91(0.06) |
| 311 | 8.16 | 8.09 | 8.05±0.07 | 8.03(0.02) | 8.17 | 8.24(0.06) |
| 400 | 7.51 | 7.53 | 7.40±0.14 | 7.40(0.02) | 7.51 | 7.45(0.09) |
| 331 | 7.18 | 7.35 | 7.32±0.12 | 7.30(0.01) | 7.52 | 7.25(0.03) |
| 422 | 6.70 | 6.81 | 6.72±0.06 | 6.74(0.00) | 7.02 | 6.76(0.02) |
| 511 | 6.44 | 6.54 | 6.40±0.08 | 6.44(0.01) | 6.65 | 6.45(0.03) |
| 333 | 6.44 | 6.50 | 6.43±0.08 | 6.46(0.01) | 6.65 | 6.53(0.06) |
| 440 | 6.03 | 6.16 | 6.04±0.15 | 6.07(0.00) | 6.18 | 6.10(0.01) |
| 444 | 4.97 | 5.11 | 5.00±0.10 | 5.00(0.01) | 5.16 | 5.05(0.02) |
| Standard deviation | | | | 0.01 | | 0.3 |
| $\|F(222)\|$ | | 0.44 | 0.44±0.08,[a] 0.41±0.01[c] | 0.47(0.04) | | 0.03(0.2) |
| $\|F(622)\|$ | | | | 0.001(0.001) | | |
| $a_0$ | | | | 1.49(0.15) | | 2.5(0.3) |
| $a_1(a_0, b_1, b_3)$ $a_B^{-1}$ | | | | 0.06(0.09) | | −0.5(0.2) |
| $a_2(a_0, b_1, b_3)$ $a_B^{-1}$ | | | | −0.005(0.003) | | 0.015(0.007) |
| $b_1$ $a_B^{-1}$ | | | | −0.24(0.02) | | −0.21(0.15) |
| $b_3$ $a_B^{-1}$ | | | | 0.8(0.1) | | −0.1(0.5) |

[a]Reference 1
[b]Reference 13.
[c]J. B. Roberto and B. W. Batterman, Phys. Rev. B 2, 3220 (1970).

state. Only the form factors $f(111)$, $f(200)$, $f(220)$, and $f(222)$ of Table I have a valence contribution outside the range of the experimental errors. The standard deviation $\sigma$ of model-vs-experimental form factors is therefore calculated for these four values. For the measurements of Ref. 10, $\sigma \approx 0.04$, while for a set proposed by Weiss,[4] $\sigma \approx 0.11$; the former set is therefore considered more accurate.

Hartree-Fock wave functions[11] in the $3s^2 3p$ configuration are used to calculate the Al atomic charge distribution $\rho(r)$.

The electron distribution in {110} planes resulting from the Raccah and Henrich data is shown in Fig. 1, core and valence distributions having been combined. The upper numbers show the result of changing cutoff value; the one at the left-hand side is for $D=26.95a_B$, the one at the right-hand side is $D=5.26a_B$. The lower numbers result from a superposition of atoms. It is apparent that in the solid, charge has moved from the vicinity of the cores to the voids between atoms. Minima occur at the midpoint of the cubic cell and equivalent points. A comparison can be made, in the region where the core distribution is negligible, with the valence distribution obtained by Harrison[12] from orthogonalized-plane-wave (OPW) form factors. Harrison's charge distribution reaches a minimum of 0.11 electrons/Å$^3$ compared to 0.15, 0.11, and 0.10 electrons/Å$^3$, at the same location, for $D=26.95a_B$, $D=5.26a_B$, and atomic superposition, respectively.

No recent experimental data for diamond are available. Measurements of Göttlicher and Wölfel[13] and of Brill *et al.*[14] are compared. These room-temperature measurements were reduced to $T=0$ °K by means of Eq. (20) with $B=0.2002 \pm 0.0001$ and $0.208 \pm 0.001$, respectively. They are not in very good agreement, as may be seen from Table II. The error bounds of Ref. 13 seem overly optimistic. According to a recent publication[1] an accuracy of 1% is about the best that can presently be obtained when measuring form factors. Fitting the Göttlicher and Wölfel data with only two parameters, $a_0$ and $b_3$, results in poor agreement with Renninger's[15] measured value for $|F(222)|$. Of the 23 tabulated form factors, only the first 11 contain valence charge contributions larger than this error limit, so that the fit is effective for these 11 values. Fitting with three parameters $a_0$, $b_1$, and $b_3$ results in $\sigma=0.02$ and $|F(222)|=0.19$ as compared with Renninger's value of 0.30 and the band-structure value[1] 0.24. The fact that $a_0<1$ indicates that val-

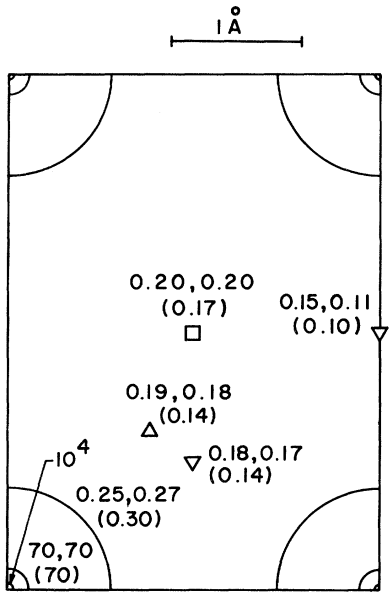


FIG. 1. Electron density (electrons/Å$^3$) in Al {110} planes derived from form factors of Ref. 1. Upper values on the left-hand side are for $D = 26.95a_B$, $a_0 = 0.1$, $a_1 = 0.35$, $a_2 = -0.013$. Upper values on the right-hand side for $D = 5.26a_B$, $a_0 = -0.1$, $a_1 = 1.02$, $a_2 = -0.19$. Values in parentheses result from superposition of atomic charge distributions. Triangle denotes a saddle point, square a maximum point, and inverted triangle a minimum point.

ence charge is pushed outward from the core region, in contradiction to the interpretation of Ref. 1. The experimental set of Brill *et al.* results in $\sigma = 0.05$, and is therefore considered the less accurate of the two. In this case, large random variations were found between measured and model form factors pertaining to higher-order reflections than those shown in Table II. The band-structure results of Ref. 1 compare better with Göttlicher and Wölfel's set of data.

Figure 2 shows the charge distribution in the {110} and {100} planes for diamond, as calculated from the Göttlicher and Wölfel model parameters. The distribution in the {110} planes differs little from that derived for room temperature by the original authors who used the method of convolution. Their charge density at the midpoint of the valence bond is 1.67 electrons/Å$^3$ as compared to 1.69 electrons/Å$^3$ in the present calculation for $T = 0\,^\circ$K; superposition of atomic charge distributions results in 1.1 electrons/Å$^3$. Just beyond the core, the site distribution has a skewed shape, as compared to the squarish shape which results from straight superposition of atoms. Outside core and bond regions the charge distribution is relatively small.

Hartree-Fock-Slater[16] atomic wave functions in the $2s2p^3$ configuration are used to calculate $\rho(r)$ of Eq. (7). Hartree-Fock[17] wave functions also were tried but they did not improve the fit.

The value $D = 12.4a_B$ is the radius to which carbon wave functions are tabulated; reducing $D$ to $4.00a_B$ causes small changes in the fitting.

For Si, two sets of measurements are compared: a set compiled by Raccah *et al.*[1,18] and one measured by Göttlicher and Wölfel.[13] The set of Ref. 13 was reduced to $T = 0\,^\circ$K using $B = 0.5021 \pm 0.0003$. Again the two-parameter model gives poor agreement with the forbidden reflection. As may be seen

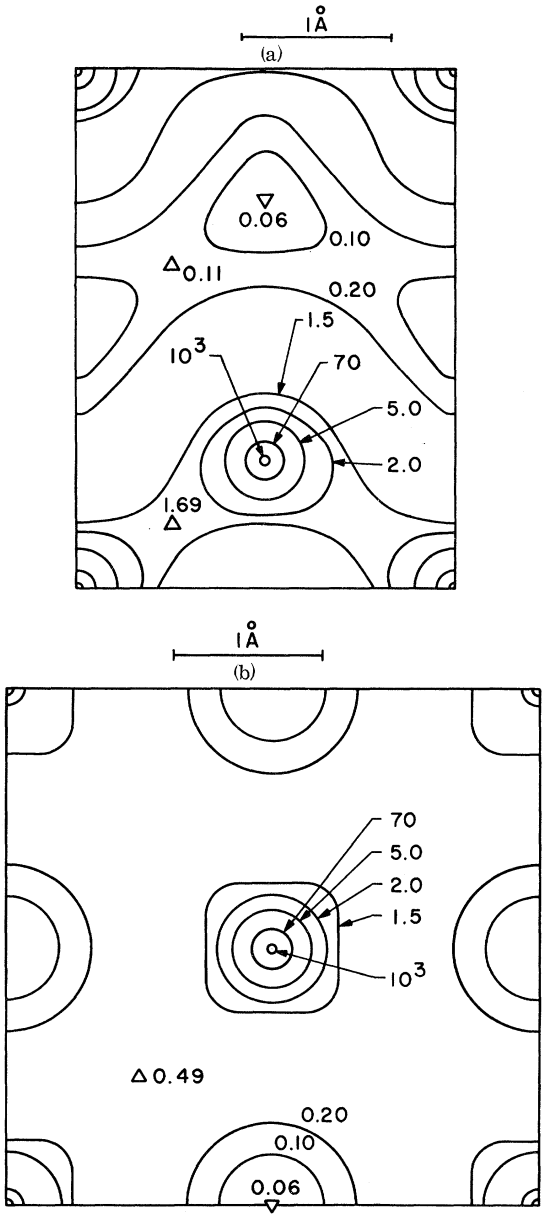


FIG. 2. Electron density (electrons/Å$^3$) in diamond derived from form factors of Ref. 13. $D = 12.4a_B$. Triangle denotes a saddle point and inverted triangle denotes a minimum point. (a) {110} planes and (b) {100} planes.

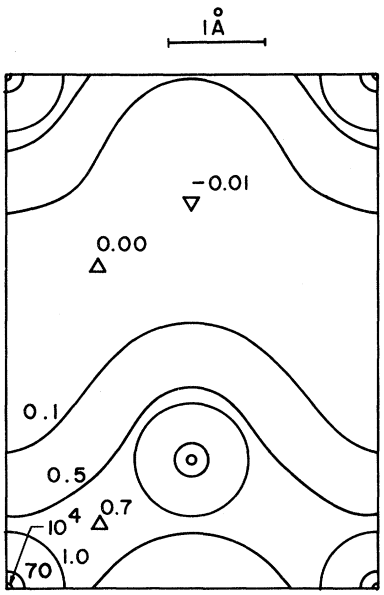


FIG. 3. Electron density (electrons/Å$^3$) in Si {110} planes derived from form factors of Ref. 1. $D = 26.3a_B$. Triangle denotes a saddle point and inverted triangle denotes a minimum point.

from Table III, the former set can be fitted quite well with the three-parameter model. Owing to the relatively large experimental errors, only the first four form factors have valence contributions larger than these. Considering only these four, we have $\sigma = 0.01$. The precision of the experimental form factors seems better than indicated. The calculated value $|F(222)| = 0.47$ is comparable with the measured value 0.44 and the band-structure value 0.44. The measurements of Göttlicher and Wölfel can not be reconciled with the model and the calculated value of $|F(222)|$ is not meaningful. This is found whether fitting to all 22 form factors or only fitting to the 10 which are listed in Table III.

The band-structure results of Ref. 1 are not in good agreement with either measured set; the discrepancy with the measurements quoted in Ref. 1 is mainly in $f(111)$. The fact that the measured set has good consistency makes it plausible that the measured $f(111)$ is correct.

Hartree-Fock wave functions[11] in a $3s3p^3$ configuration are used to generate $\rho(r)$. The $2p$ electrons overlap in the crystal, so that their charge distribution should probably be slightly readjusted; however, the form factors of Ref. 1 can be fitted without making allowance for this. Here, $D = 26.3a_B$, the radius to which the wave functions are tabulated.

The charge distribution in the {110} planes is shown in Fig. 3. Bonding is again apparent. There is less distortion in the vicinity of the nuclei than there is for diamond due to the larger core region. At the midpoint of the bond, the charge density is 0.7 electrons/Å$^3$ as compared to Göttlicher and Wölfel's 0.57-electrons/Å$^3$ room-temperature value and their value of 0.32 electrons/Å$^3$ for a superposition of Hartree atoms. The site distributions corresponding to the measurements of Ref. 18 indicate little radial redistribution; the deviation from atomic form factors is mainly due to the angular term in Eq. (7).

In the region outside core and valence bonds the charge distribution is extremely small. The negative value sets a lower bound for the probable error.

## VII. CONCLUSIONS

A parametrized model charge distribution for cubic crystals has been proposed and an expression for the corresponding form factors has been derived. By means of the latter, consistency of two sets of experimental form factors for each of Al, diamond, and Si has been examined and one has been chosen as the more reliable.

It was shown that in case of the diamond structure the tabulated quantities in the literature are not truly form factors. The relation between these quantities and the true form factors was derived. The occurrence of forbidden reflections was made plausible and an expression for their structure factors was derived.

In the application of the fitting procedure it became clear that a set of experimental form factors of relatively high precision is needed in order to establish the number of parameters that should be used in the model. The recent experimental results of Raccah and Henrich[10] for Al could be fitted without parameters.

The model may possibly serve as a test for form factors of other metals for which experimental form factors are presently available. In the case of Cr, Fe, and Cu, the $d$-electron charge could be varied.

For diamond structures it seems that the cubic term in $b_1$, as well as the tetrahedral term in $b_3$, must be included in order to obtain agreement with the experimental values of $|F(222)|$. In the case of Si, agreement between the model, experimental, and band-structure values of $|F(222)|$ is better than for diamond. A new experimental determination of the forbidden reflection of diamond would contribute to the verification of the proposed model.

## ACKNOWLEDGMENTS

The author is indebted to R. D. Scanlon for advice on, as well as for the use of his computer subroutines for, nonlinear least-squares fitting and calculation of empirical error bounds. A helpful discussion with Professor E. Brown is also acknowledged.

[1]P. M. Raccah, R. N. Euwema, D. J. Stukel, and T. C. Collins, Phys. Rev. B 1, 756 (1970).
[2]See, e.g., Charles Kittel, *Introduction to Solid State Physics*, 2nd ed. (Wiley, New York, 1956), Chap. 2.
[3]R. Hosemann and S. N. Bagchi, Nature 171, 785 (1953).
[4]R. J. Weiss, *X-ray Determination of Electron Distribution* (Wiley, New York, 1966); Phys. Letters 12, 293 (1964).
[5]At the present level of experimental accuracy, such differences can only be detected for elements of relatively low atomic number because, for large atomic number, the core contribution overshadows the valence contribution.
[6]A. Marcus Gray, Watervliet Arsenal Technical Report No. WVT-7037, 1970 (unpublished).
[7]An IBM-360-44 Computer was used for all computations.
[8]See, e.g., R. Brill, Solid State Phys. 20, 1 (1967).
[9]H. Witte and E. Wölfel [Z. Physik. Chem. NF 3, 296 (1955)] give a detailed description and both methods are applied to NaCl.
[10]P. M. Raccah and V. E. Henrich, Phys. Rev. 184, 607 (1969).
[11]Calculated from tabulated coefficients of R. E. Watson and A. J. Freeman, Phys. Rev. 123, 521 (1961).
[12]W. A. Harrison, *Pseudopotentials in the Theory of Metals* (Benjamin, New York, 1966), p. 225.
[13]S. Göttlicher and E. Wölfel, Z. Elektrochem. 63, 891 (1959).
[14]R. Brill, H. G. Grimm, C. Hermann, and Cl. Peters, Ann. Physik 34, 393 (1939).
[15]M. Renninger, Z. Krist. Mineral. (Petrograd) 97, 107 (1937); Acta Cryst. 8, 606 (1955).
[16]F. Herman and S. Skillman, *Atomic Structure Calculations* (Prentice-Hall, Englewood Cliffs, N. J., 1963).
[17]A. Jucys, Proc. Roy. Soc. (London) A173, 59 (1939).
[18]In this set $f(111)$ and $f(222)$ are measurements of L. D. Jennings, J. Appl. Phys. 40, 5038 (1969); $f(220)$ is a measurement of M. Hart and A. D. Milne, Acta Cryst. A 25, 134 (1969); all other measurements are by H. Hattori, H. Kuriyama, and N. Kato, J. Phys. Soc. Japan 20, 1047 (1965).

PHYSICAL REVIEW B VOLUME 5, NUMBER 2 15 JANUARY 1972

# Theory of the de Haas–van Alphen Effect in Dilute Alloys*

Paul Soven†
*Department of Physics and the Laboratory for Research on the Structure of Matter, University of Pennsylvania, Philadelphia, Pennsylvania* 19104
(Received 16 August 1971)

Multiple-scattering theory is employed to determine the one-electron Green's function in the presence of a uniform external magnetic field and a dilute random arrangement of atomic potentials. The oscillatory part of the density of states is extracted and used to compute thermodynamic quantities. Explicit expressions for the frequency shifts and the amplitude diminution caused by inserting impurities into the free-electron gas are obtained.

## I. INTRODUCTION

The de Haas–van Alphen (dHvA) effect has long been a useful tool for the investigation of extremely pure metals. In recent years it has been applied to the study of controlled dilute alloys in an attempt to elucidate the electronic properties of these relatively simple disordered materials.[1] One is primarily interested in the effect of alloying on the frequency of the dHvA oscillations, since this quantity depends directly upon the electronic states in the vicinity of the Fermi energy.

There have been several theoretical studies of the dHvA effect in dilute alloys. The earliest was the pioneering work of Dingle,[2] which was essentially a phenomenological treatment of the effect of impurity scattering on the amplitude of the oscillations. Dingle argued that the result of such scattering was to broaden the Landau levels (the quantized energy levels of an electron in a spatially uniform magnetic field). Since the dHvA effect arises from the passage of such levels through the chemical potential of the system, the broadening of the otherwise sharp levels manifests itself as a diminution in the amplitude of the oscillations. While correct in spirit, Dingle's treatment gave no prescription for calculating the lifetime causing the decrease in amplitude. Furthermore, it did not deal with the frequency shifts produced by alloying. Heine[3] did consider the question of what would happen to the frequency as impurities were added to the perfect crystal. His approach was a fundamental one, insofar as the effects of alloying in the absence of an external field were concerned, but did not attempt to deal with field-dependent effects in a basic way.

Bychkov[4] attempted to apply multiple-scattering theory to the problem. His work was limited to the case of a zero-range potential, and in any event was not concerned with the questions of frequency shifts. His expressions for the lifetime associated with the dHvA oscillations differ from those derived here and in Ref. (5) by the presence of apparently extraneous factors. Brailsford[5] discussed the question of frequency changes and amplitude reduction using what was essentially a ruse to avoid